~~15 Years of~~ Science with XMM-Newton:
Selected Highlights from the last 2 years

Matthias Ehle, Norbert Schartel
XMM-Newton SOC, European Space Astronomy Centre, Madrid
20 November 2014

XMM-Newton Launch on 10 December 1999

Spacecraft and Mirrors

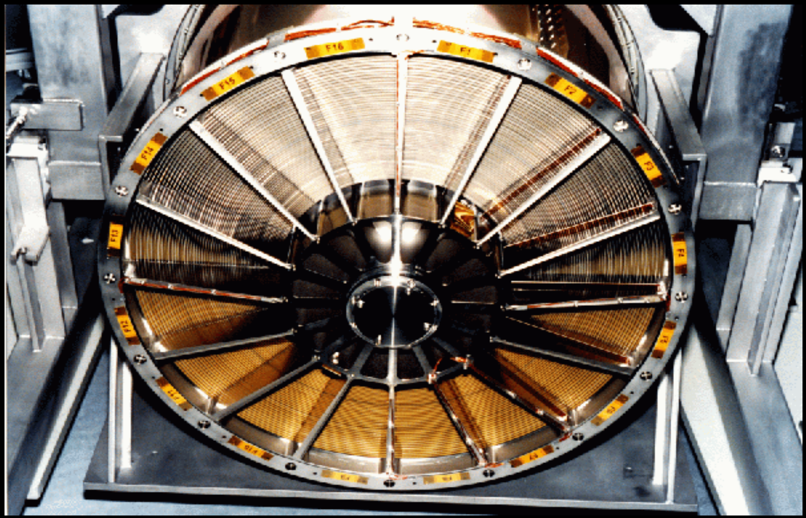

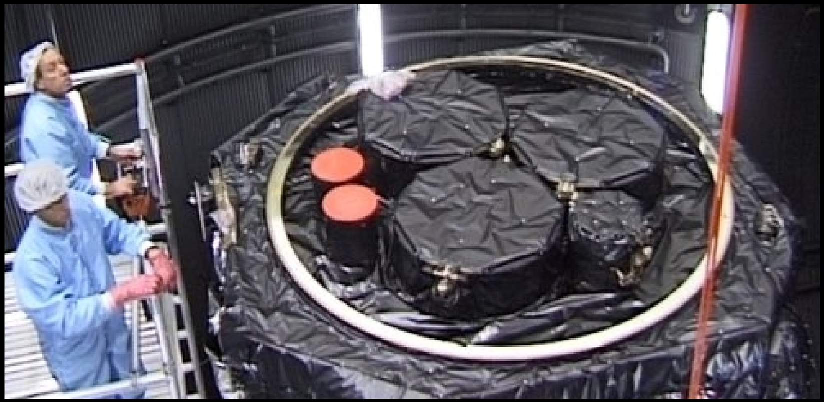

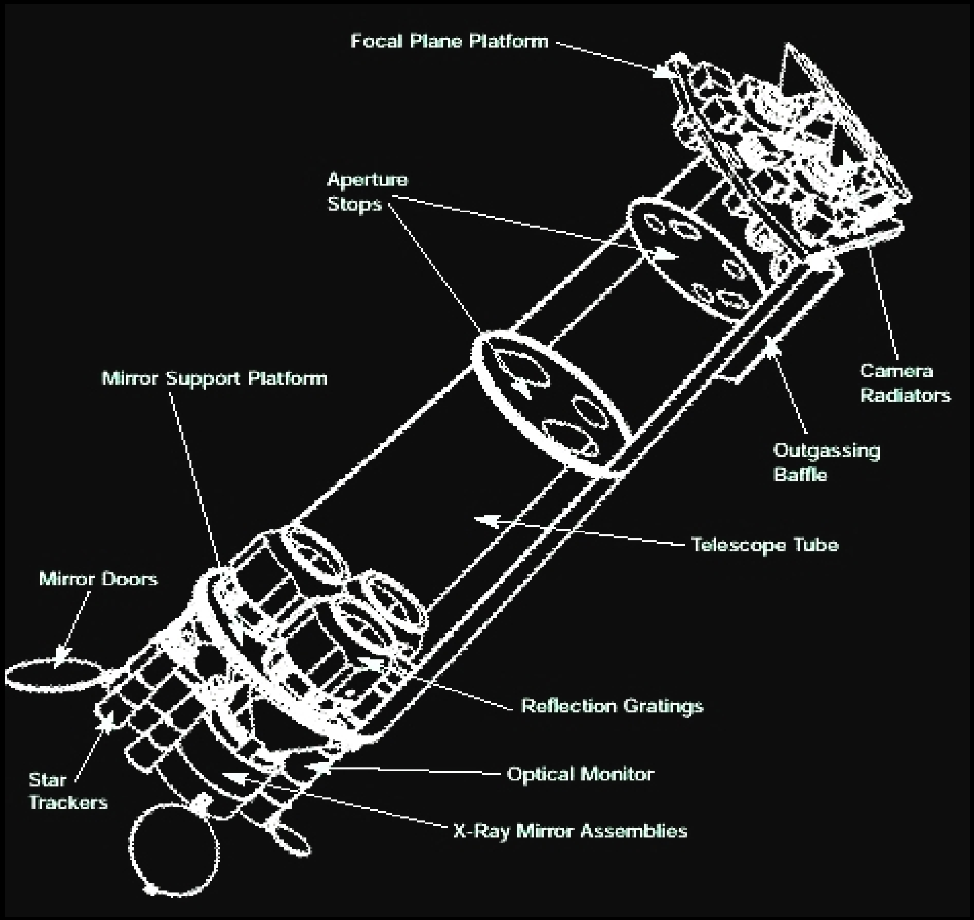

Instruments

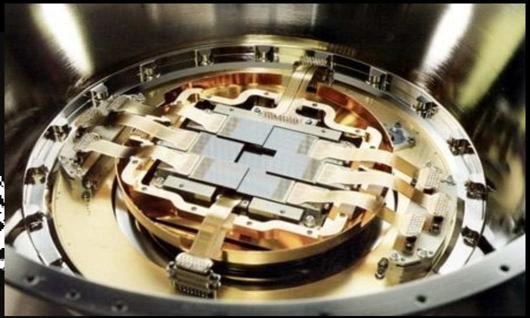

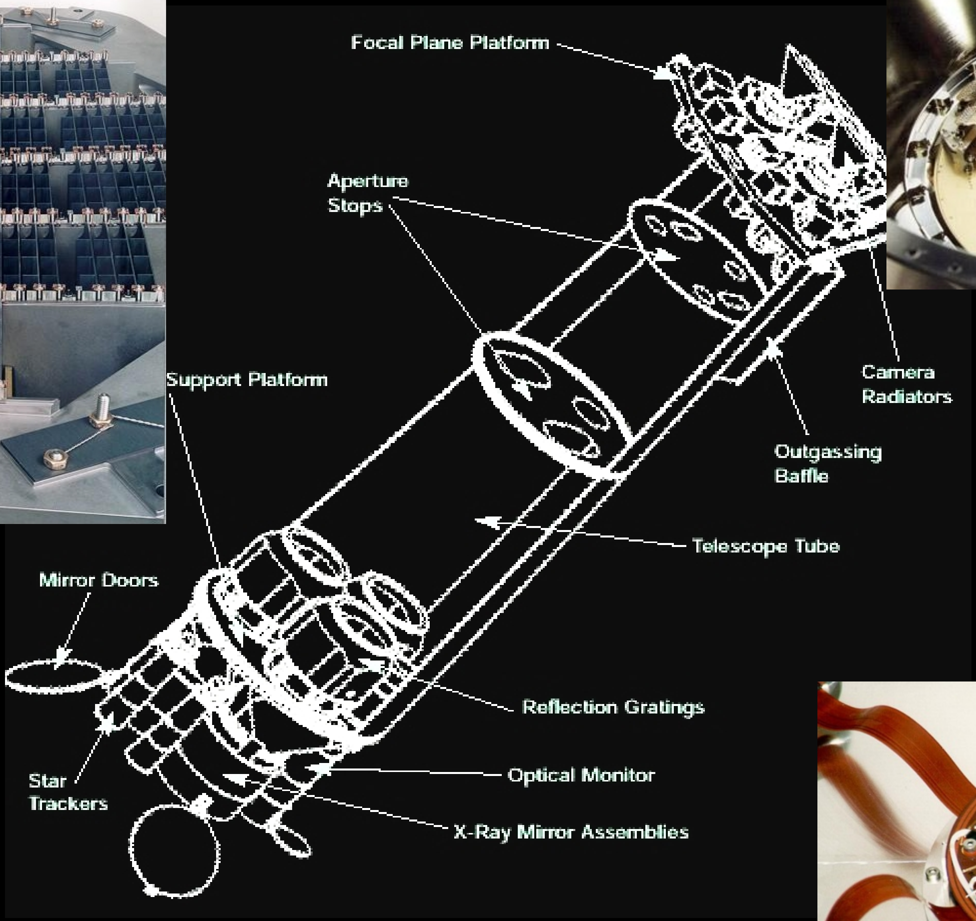

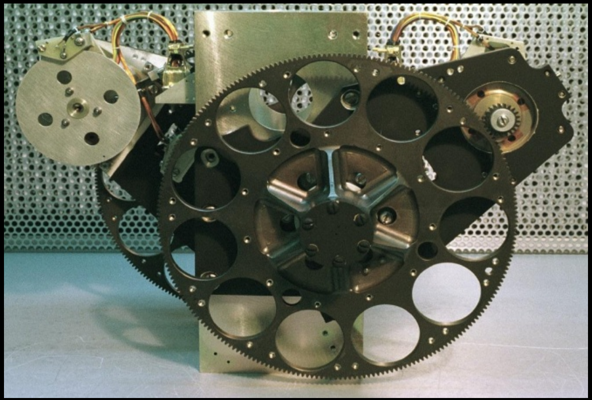

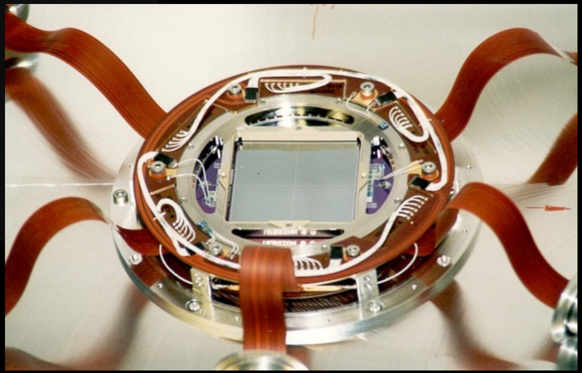

XMM-Newton

- 3 Mirror Modules / highest effective collecting area ever
- Six simultaneously observing instruments:
  - 3 CCD cameras (one pn and two MOSs)
  - 2 spectrometers (RGS)
  - 1 optical Monitor (OM)

Some Scientific Highlights from the last two years...

The Corona of HD 189733 Flares in Phase With Exoplanet's Orbit

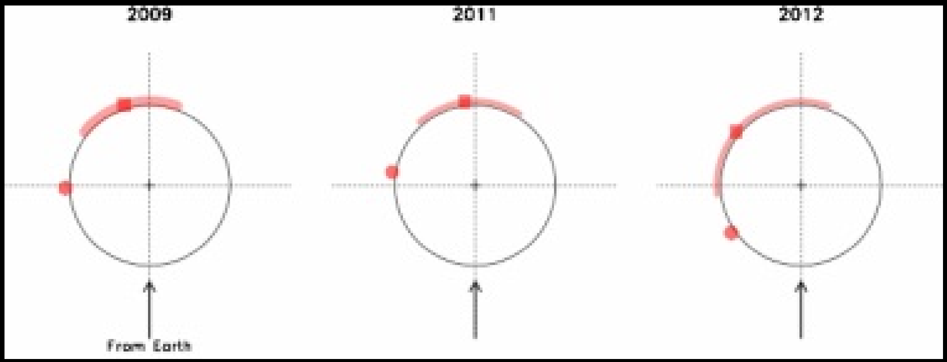

Planetary phases observed in 2009, 2011, and 2012

Pillitteri, et al., 2014, ApJ 785, 145

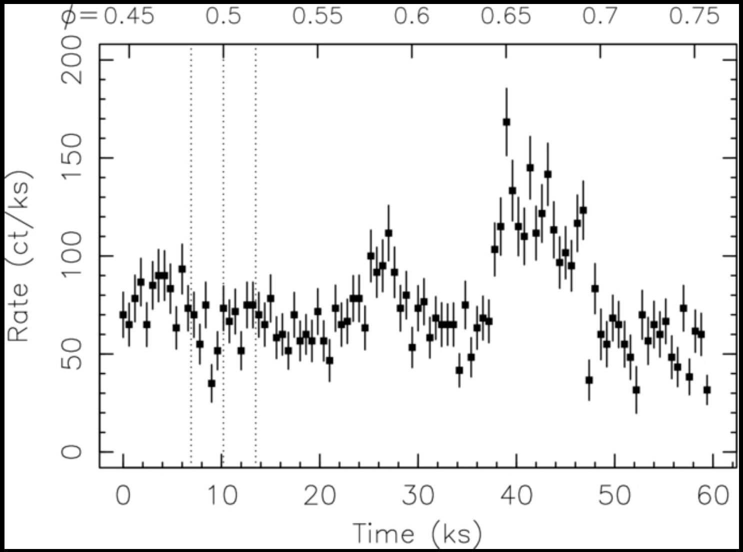

EPIC-pn light curve of HD 189733

HD 189733 has a close-in, transiting, massive exoplanet (hot Jupiter)

➔ Flares in 2009, 2011 and 2013 restricted to a small planetary phase range of $\Phi = 0.55$-0.65

➔ Quiescent spectrum: two temperatures at 0.2 keV and 0.7 keV

➔ During the flares a third component at 0.9 keV

➔ Flaring structure as big as four stellar radii.

➔ Magnetic field in this loop: 40 - 110 G

➔ The large length suggests an origin due to magnetic interaction between the star and the close-in planet.

➔ The magnetic field associated with the planet exerts a force on the plasma and the coronal loop when the planet passes close to regions of the stellar surface

Discovery of X-Ray Pulsations from the Massive Star ζ^1 CMa

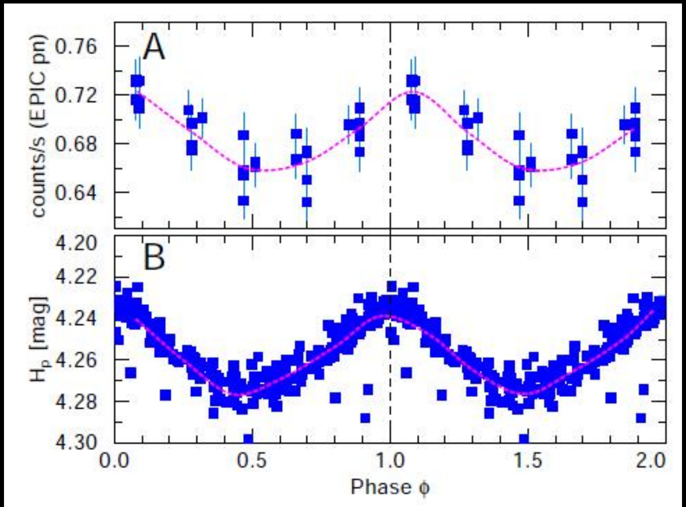

A: X-ray light curve (0.2-10.0keV)
B: the Hipparcos Catalogue Epoch Photometry data

Massive stars drive fast stellar winds where shocks can develop

➔ X-rays from shock-heated plasma

➔ Many massive stars pulsate

➔ It was neither theoretically predicted nor observed that these pulsations would affect the X-ray emission.

Oskinova, et al., 2014, NatCo 5E4024O

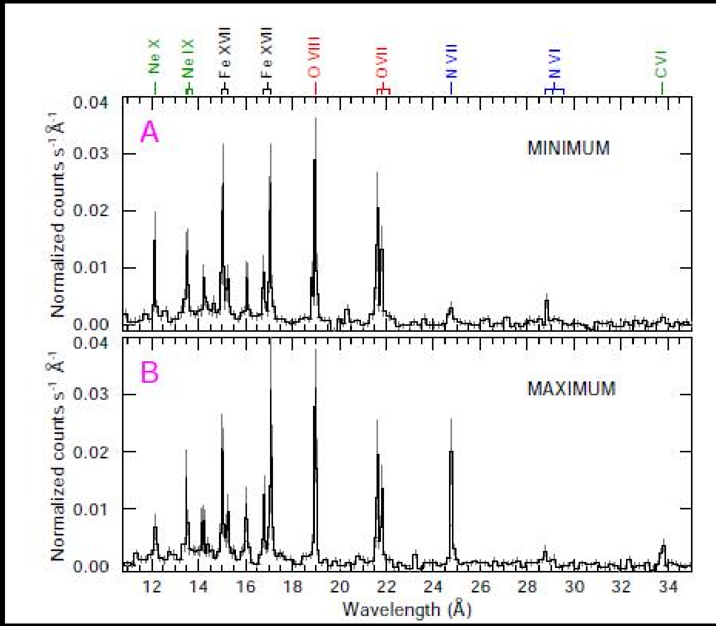

Phase dependent RGS spectra

The massive B-type star ζ^1 CMa is a variable of Cep type and has a strong magnetic field. XMM-Newton observations reveal:

➔X-ray pulsations with the same period (P = 4.90±0.09 h) as the fundamental stellar oscillations.

➔ plasma heating and cooling

➔ X-ray emitting plasma is located close to the photosphere

This discovery challenges our understanding of stellar winds from massive stars, their X-ray emission, and their magnetism.

Synchronous X-ray and Radio Mode Switches: A Rapid Global Transformation of the Pulsar Magnetosphere

Simultaneous observations of PSR B0943+10 with XMM-Newton and GMRT and LOFAR:

➔ Detection of synchronous switching in the radio and x-ray emission properties

➔ When the pulsar is in a sustained radio-"bright" mode, the x-rays show only an unpulsed, nonthermal component

➔ When the pulsar is in a radio-"quiet" mode, the x-ray luminosity more than doubles and a 100% pulsed thermal component is observed along with the nonthermal component.

➔ Indicates rapid, global changes to the conditions in the magnetosphere, which challenge all proposed pulsar emission theories.

Hermsen, et al., 2013
Science 339, 436

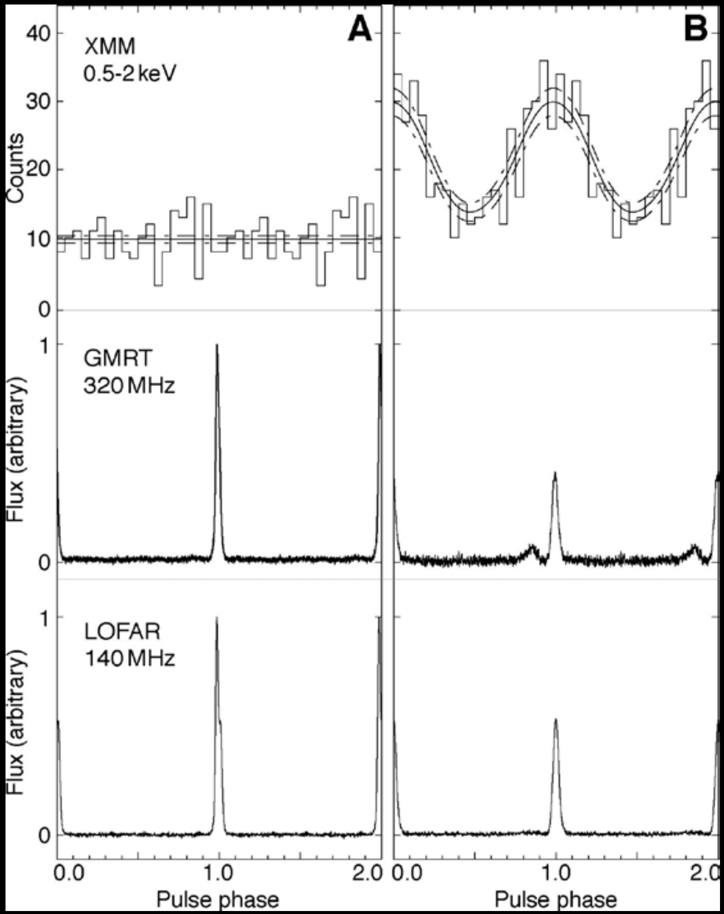

Aligned x-ray and radio pulse profiles of PSR B0943+10 in its B and Q modes. (A) B mode: There is no evidence for a pulsed signal in the B-mode x-ray data, the flat distribution showing constant emission from the pulsar. (B)Q mode: The x-ray profile in the Q mode represents a 6.6s detection on top of a flat constant level

Swings between Rotation and Accretion Power in a Binary Millisecond Pulsar

- XMM-Newton, radio and other X-ray satellites observations of X-ray transient IGR J18245–2452, which was first detected by INTEGRAL
- First observations of accretion-powered, millisecond X-ray pulsations from a neutron star previously seen as a rotation-powered radio pulsar.
- Within a few days after a month-long X-ray outburst, radio pulses were again detected.

➔ evolutionary link between accretion and rotation-powered millisecond pulsars

➔ some systems can swing between the two states on very short timescales

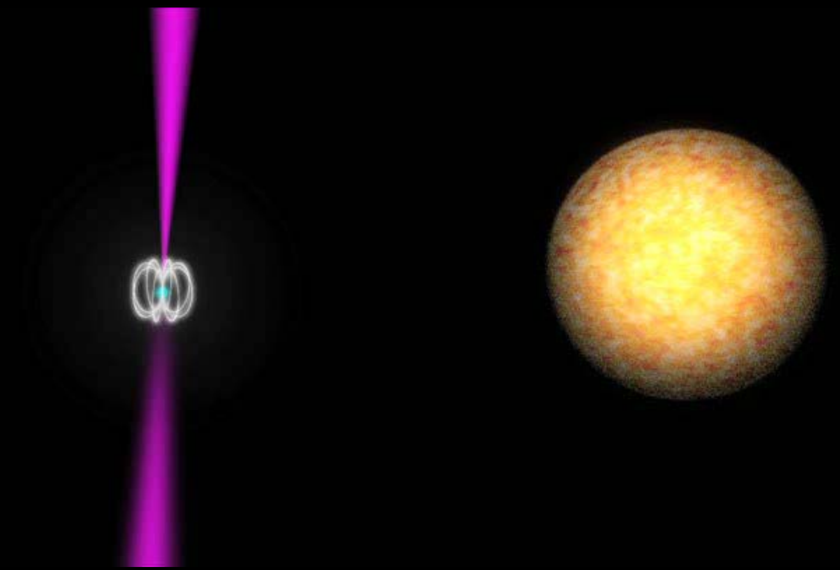

Fourier power spectral density of the 0.5–10-keV X-ray photons observed by the EPIC pn camera. The peaks at 254.3 and 508.6 Hz represent the first and second harmonics of the coherent modulation of the X-ray emission of IGR J18245–2452.

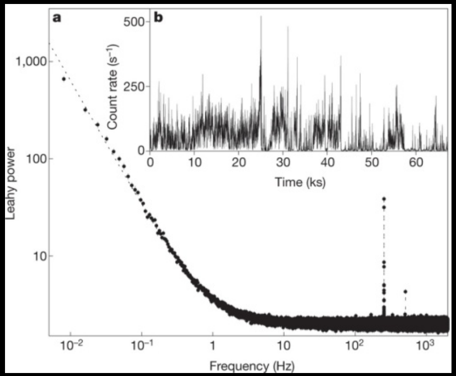

Papitto, et al., 2013, Nature 501, 517

Magnetic Multipole Field in SGR 0418+5729

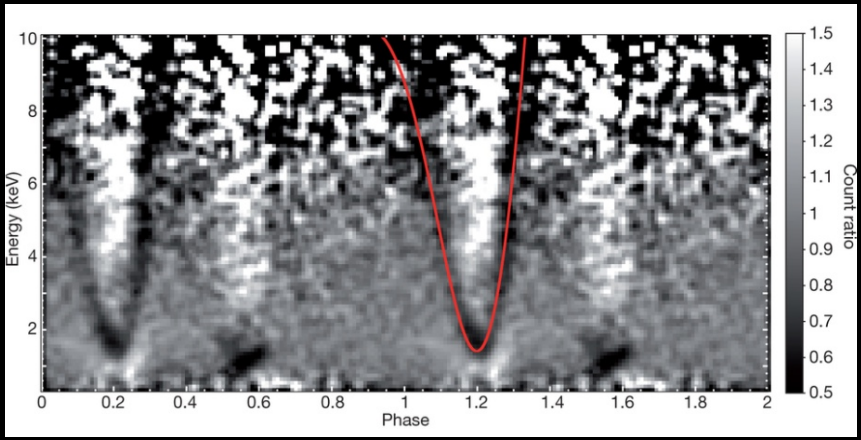

Phase-dependent spectral feature in the EPIC data of SGR 0418+5729.

- Soft-γ-ray repeaters (SGRs) and anomalous X-ray pulsars (AXPs) are neutron stars that sporadically undergo X-ray/γ outbursts
- sources are mainly powered by their own magnetic energy
- magnetic fields inferred from several observed properties of SGRs and AXPs are greater than those of radio pulsars

SGR 0418+5729 has a weak dipole magnetic moment of B = 6×10^{12} G (derived from timing parameters).

A strong field has been proposed in the stellar interior and in multipole components on the surface.

➔ X-ray absorption line which depends strongly on the star's rotational phase

➔ proton cyclotron magnetic field from 2×10^{14} G to 10^{15} G

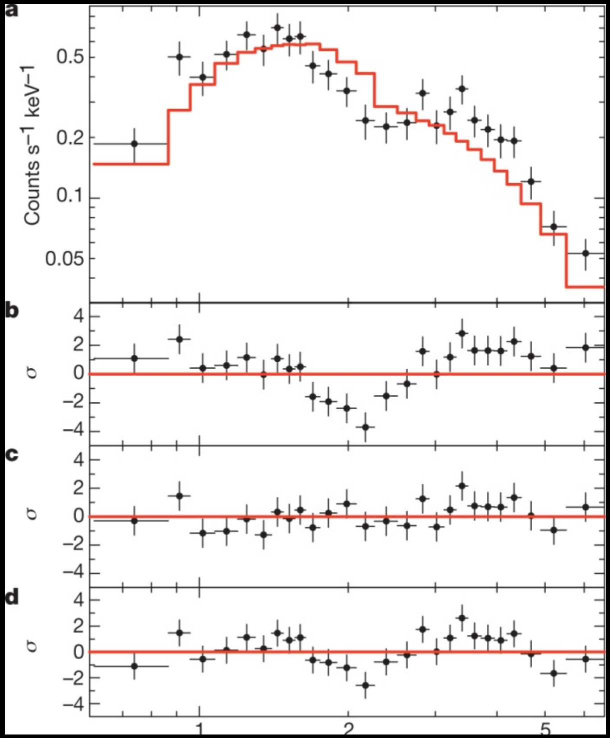

a: spectrum from phase interval 0.15–0.17 and phase-averaged spectrum in red
b: residuals; c: residuals after adding an absorption line

Tiengo, et al., 2013, Nature 500, 312

Baryons in the Relativistic Jets of the Stellar-mass Black-Hole 4U 1630-47

- Accreting black holes power relativistic jets
- The power of the jets depends strongly on their composition
- Energetic considerations and circular-polarization measurements provide conflicting evidence for the presence or absence of baryons in jets (only exception peculiar X-ray binary SS 433)

➔ Detection of Doppler-shifted X-ray emission lines from a black-hole candidate X-ray binary 4U 1630-47

➔ Coincident with the reappearance of radio emission from the jets of the source

➔ Lines arise from baryonic matter in a jet travelling at ~2/3 speed of light, thereby establishing the presence of baryons in the jet

➔ Such baryonic jets are more likely to be powered by the accretion disk than by the spin of the black hole

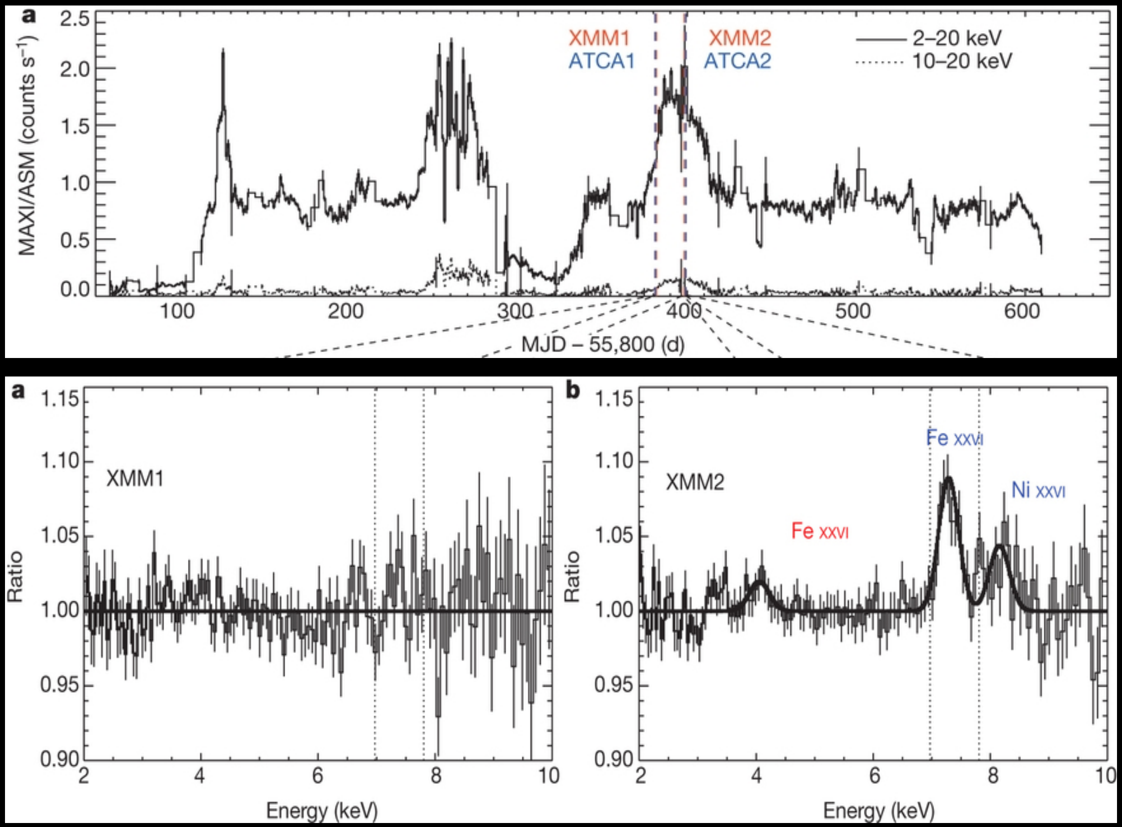

Diaz Trigo, et al., 2013, Nature 504, 260

A Rapidly Spinning Supermassive Black Hole at the Centre of the galaxy NGC 1365

Simultaneous observation of NGC 1365 by XMM-Newton and NuSTAR:

- ➔ relativistic disk features through broadened Fe-line emission and an associated Compton scattering excess at 10-30 keV
- ➔ temporal and spectral analyses allow to disentangle continuum changes due to time-variable absorption from reflection, which arises from a region within 2.5 gravitational radii of the rapidly spinning black hole
- ➔ Absorption-dominated models that do not include relativistic disk reflection can be ruled out both statistically and on physical grounds

Risaliti, et al., 2013, Nature 494, 449

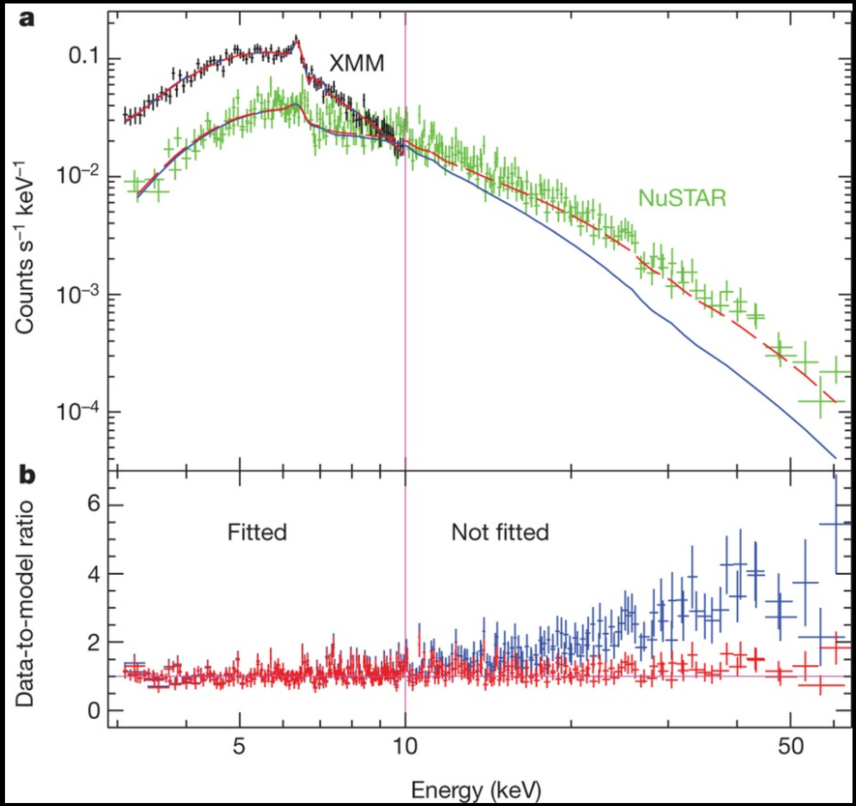

a: XMM-Newton and NuSTAR spectral data and models, b: Data-to-model ratio. The two models contain either a relativistic reflection component plus variable partial covering (red), or a double partial covering (blue). Both models have been fitted to the data below 10 keV, and reproduce the lower-energy data well. However, the models strongly deviate at higher energies.

Reflection from the strong gravity regime in a quasar at redshift z = 0.658

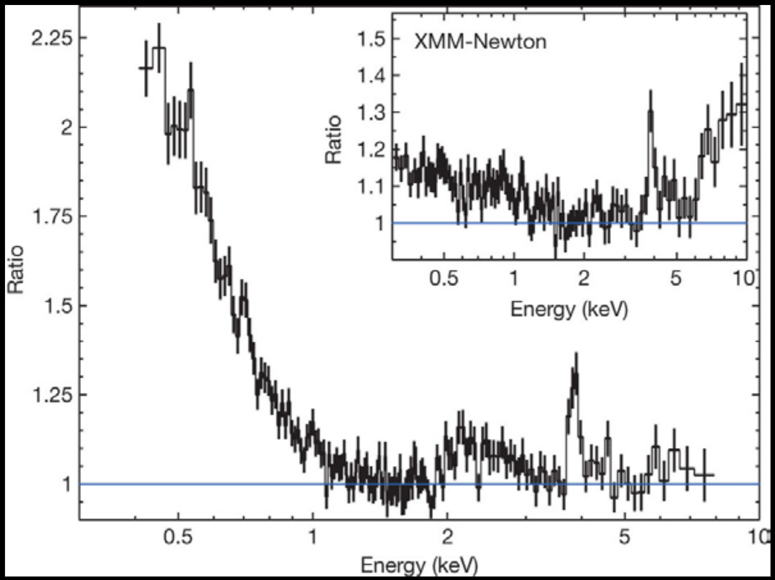

Reis, et al., 2014, Nature 507, 207

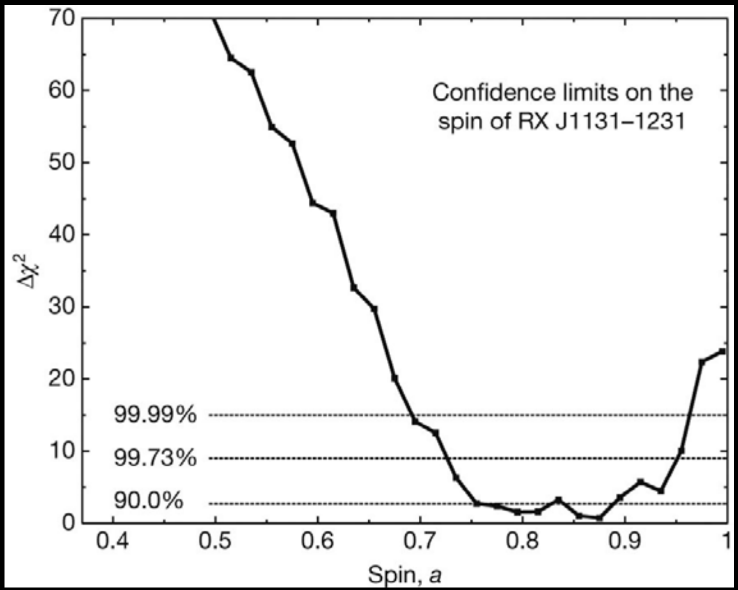

➔ **The emission originates within three gravitational radii from the black hole, implying a spin parameter of a = $0.87^{+0.08}_{-0.15}$ at the 3σ confidence level and a > 0.66 at the 5σ level.**

➔ **The high spin is indicative of growth by coherent accretion for this black hole, and suggests that black-hole growth at 0.5 <= z <= 1 occurs principally by coherent rather than chaotic accretion episodes.**

The Structure of the Milky Way's Hot Gas Halo

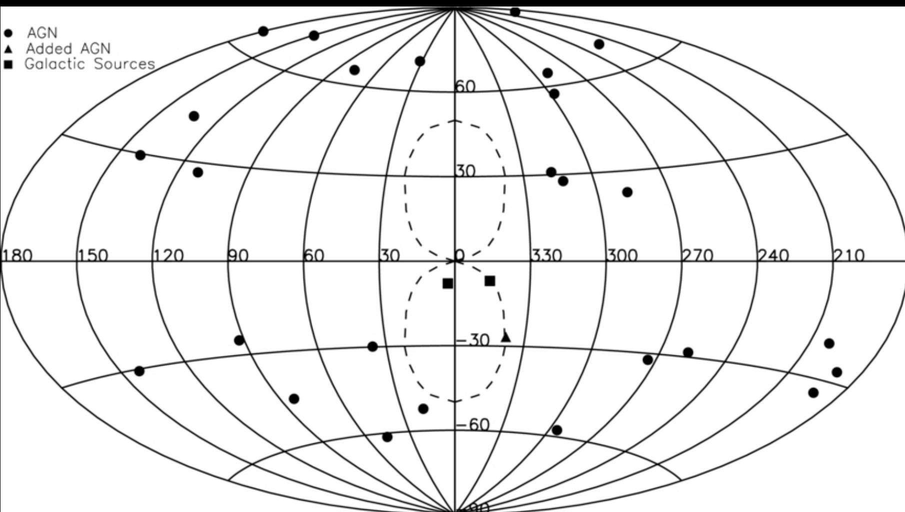

Distribution of X-ray absorbing lines of sight on the sky

Miller & Bregman, 2013, ApJ 770, 118

The Milky Way's hot gaseous halo contains a considerable amount of mass that, depending on its structural properties, can be a significant mass component.

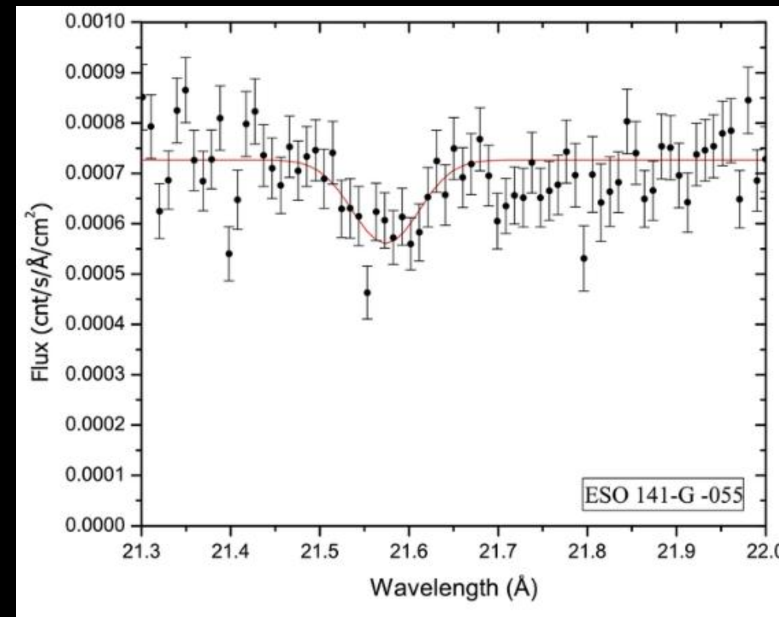

XMM-Newton flux at 21.6 to show Ovii absorption.

➔ XMM-Newton Reflection Grating Spectrometer archival data measure O VII Kα absorption-line strengths toward 26 AGN, LMC X-3, and two Galactic sources

➔ assume a β-model as the underlying gas density profile

➔ halo masses between M(18 kpc) = $7.5^{+22.0}_{-4.6} \times 10^{8}$ Mo and M(200 kpc) = $3.8^{+6.0}_{-0.5} \times 10^{10}$ Mo assuming a metallicity of Z = 0.3 Zo

➔ maximum obtained baryon fraction of fb = $0.07^{+0.03}_{-0.01}$ is significantly smaller than the universal value of fb = 0.171

➔ the mass contained in the Galactic halo accounts for 10%-50% of the missing baryons in the Milky Way.

Detection of An Unidentified Emission Line in the Stacked X-Ray Spectrum of Galaxy Clusters

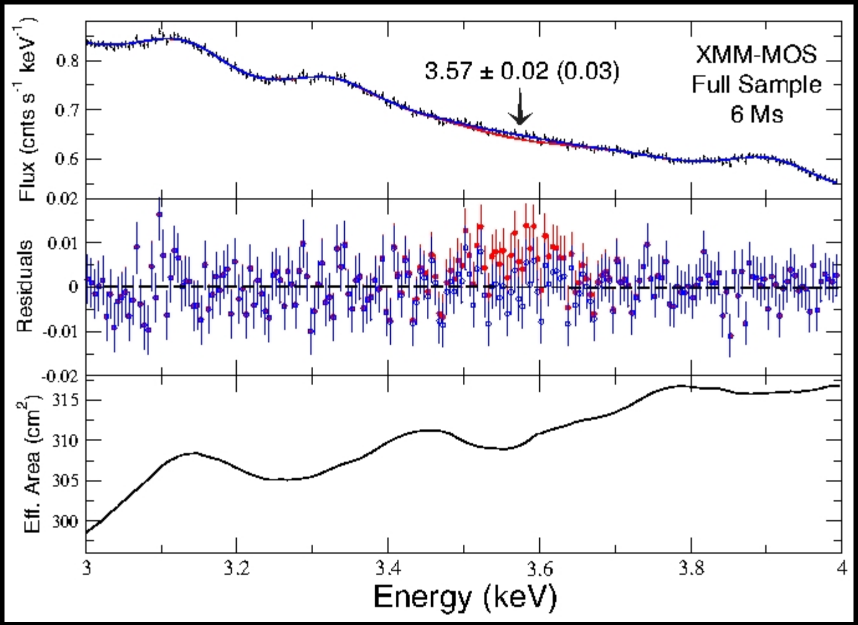

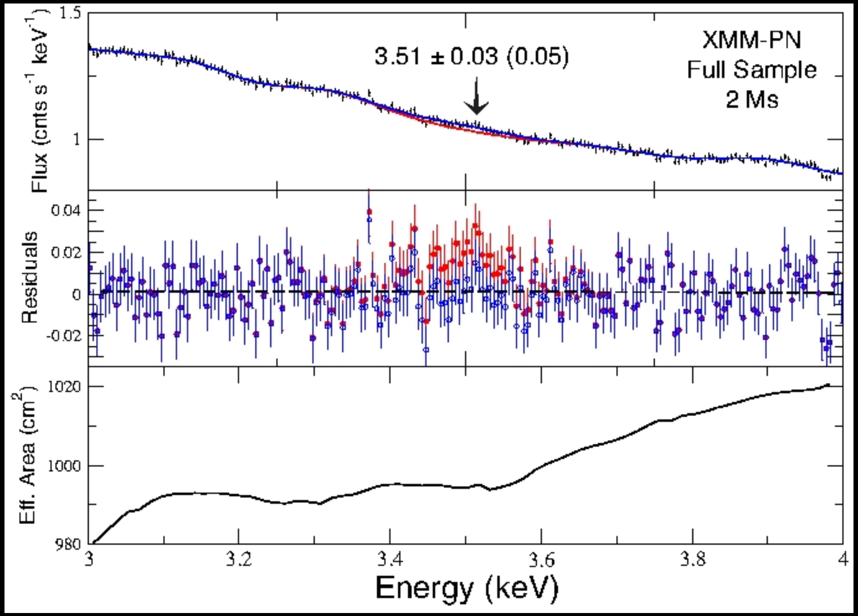

➔ weak unidentified emission line at E= 3.56+/-0.03 keV in the stacked XMM spectrum of 73 galaxy clusters spanning a redshift range 0.01-0.35.

➔ no atomic transitions in thermal plasma at this energy

Bulbul, et al., 2014, ApJ 789, 13
Boyarsky, et al., 2014, arXiv1408.2503B and arXiv1402.4119B

➔ an intriguing possibility is the decay of sterile neutrino, a long-sought dark matter particle candidate

➔ assuming that all dark matter is in sterile neutrinos with m = 2E = 7.1 keV, the detection corresponds to a neutrino decay mixing angle $\sin^2(2\theta)=7 \times 10^{-11}$

➔ below previous upper limits

Happy Birthday Chandra!!!

From your friends and colleagues at the XMM-Newton SOC.

Our best wishes for the future (science).